High Energy Density and High Intensity Physics

Low divergence electron beams from a gas cell

We report on the generation of electron beams with unusually low divergences. The beams were produced by laser wakefield acceleration in a gas cell, which typically produces high quality beams, but with a large divergence due to the strong focusing fields present in the plasma. By using a gas cell with a shaped exit aperture, the transition between the plasma and the vacuum was smoothed, resulting in improved transverse beam properties. Measurements from the electron spectrometer indicate divergences of approximately 0.2 mrad, while higher resolution measurements made using image plate suggest that the true resolution was lower than this, reaching a minimum of 0.04 mrad. These results are of interest for many potential applications where transverse beam quality is paramount, such as for light sources and for staged acceleration.

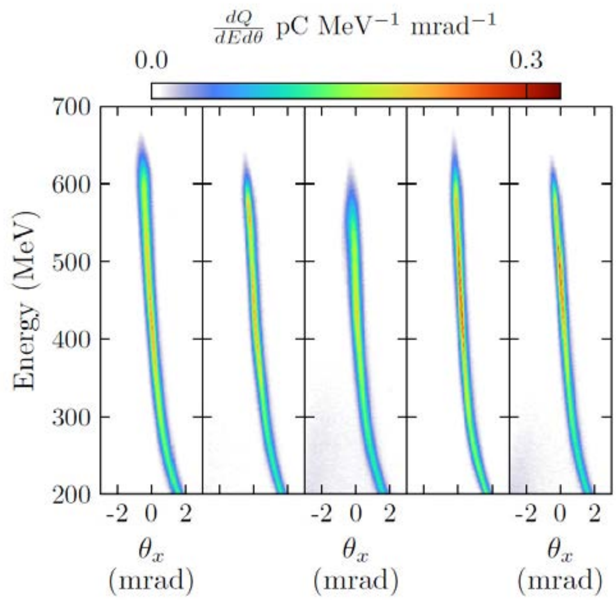

Figure 1: Sequential electron beam spectra highlighting the low divergence of the beams.

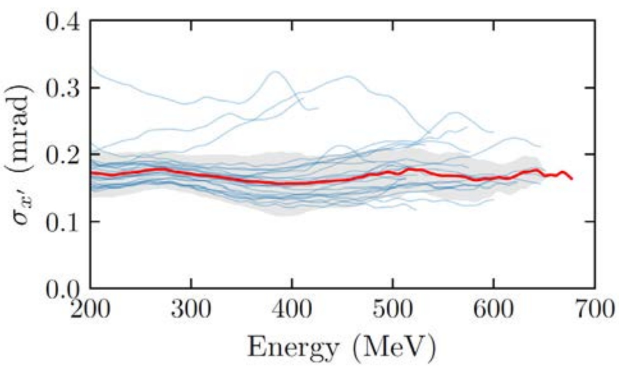

Figure 2: Energy resolved divergence measurements. The blue lines are the measurements for each spectrum in the data set, the red line is the median, and the shaded region is the standard deviation.

Authors: **M.P. Backhouse**, R. Luo, J. Hills, L. Kennedy, C. Cobo, E. Los, Z. Najmudin, N. Lopes, E. Gerstmayr, J. Sarma, N. Bourgeois, D. Bloemers, A. Thomas, S. Hawkes, S. Dann

Beam driven electron acceleration to 4 GeV at Gemini

We present measurements of electrons accelerated to high energies using both arms of the Gemini laser system. The experiment used a pair of gas cells, where the first cell acted as an injector stage, producing electron beams with peak energies of approximately 1 GeV, and the second cell provided a secondary energy boost. The boost could be large enough to approach the measurement limit of the magnetic spectrometer used, at 4.0 GeV. The modulation of the spectrum due to the plasma in the second cell is consistent with beam driven acceleration, making this experimental setup an example of the LWFA-PWFA hybrid accelerator concept. These results have implications for future implementations of LWFA seeded beam driven plasma accelerators.

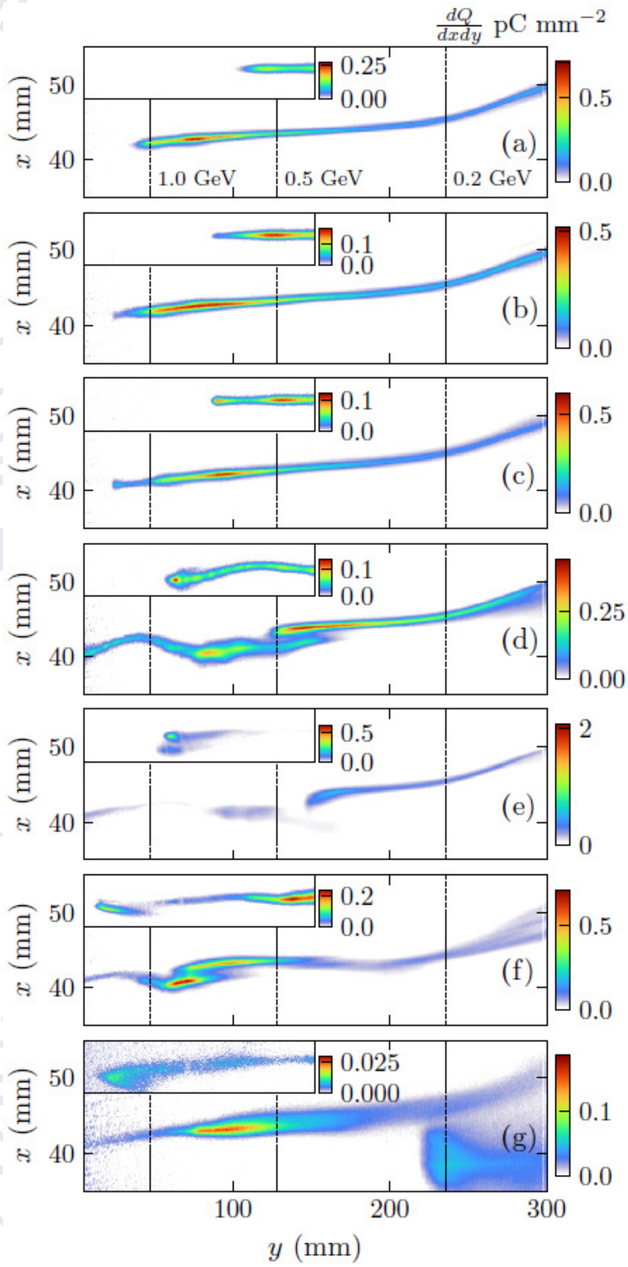

Figure 1 (left): Example images from the electron spectrometer screens. The main panels show images from the lower energy screen while the inset shows the measurements from the higher energy screen. Panels (a-c) show electron spectra after generation in cell 1. Subplots (d-g) show beams after propagating through the plasma in the second cell, resulting in an energy boost for some electrons and transverse modulations of the beam.

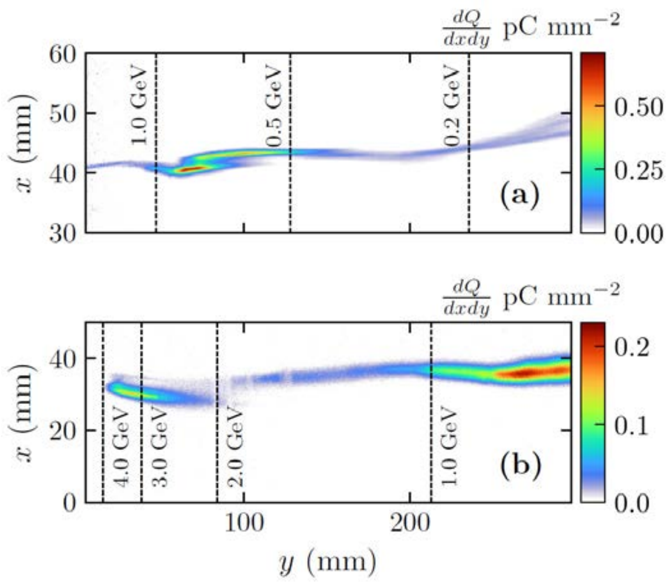

Figure 2 (above): Electron spectrometer images with overlaid energy contours from a shot where a large gain of energy was observed due to the second cell.

Authors: **M.P. Backhouse** ✉, R. Luo, J. Hills, L. Kennedy, C. Cobo, E. Los, Z. Najmudin, N. Lopes, E. Gerstmayr, J. Sarma, G. Sarri, P. Blum, R.J. Shalloo, N. Bourgeois

Plasma mirror operation at high intensity: Reflectivity and beam profile

Reflectivity and reflected beam profile from a plasma mirror at high incident intensities (on the order of $10^{19} - 10^{21}$ Wm^{-2}) was characterised for the Gemini North beam incident on 125 µm thick Kapton tape. Post-reflection pointing was characterised with an additional pointing variation of θ_{av} = 2.6 mrad generated by the formation of the plasma mirror. Adjusting focal spot area on the tape and pulse energy allowed for on-tape intensity variation. A maximum reflectivity above 70% was observed with a drop off for intensities nearing 3 x 10^{21} Wm^{-2}. Focusing further from the tape resulted in a lower quality of reflected spot at comparable intensities, with less energy contained within the FWHM (20% compared to 10% at 10^{21} Wm^{-2}). The results presented highlight important areas for development and optimal operation regimes of plasma mirrors for future staging applications.

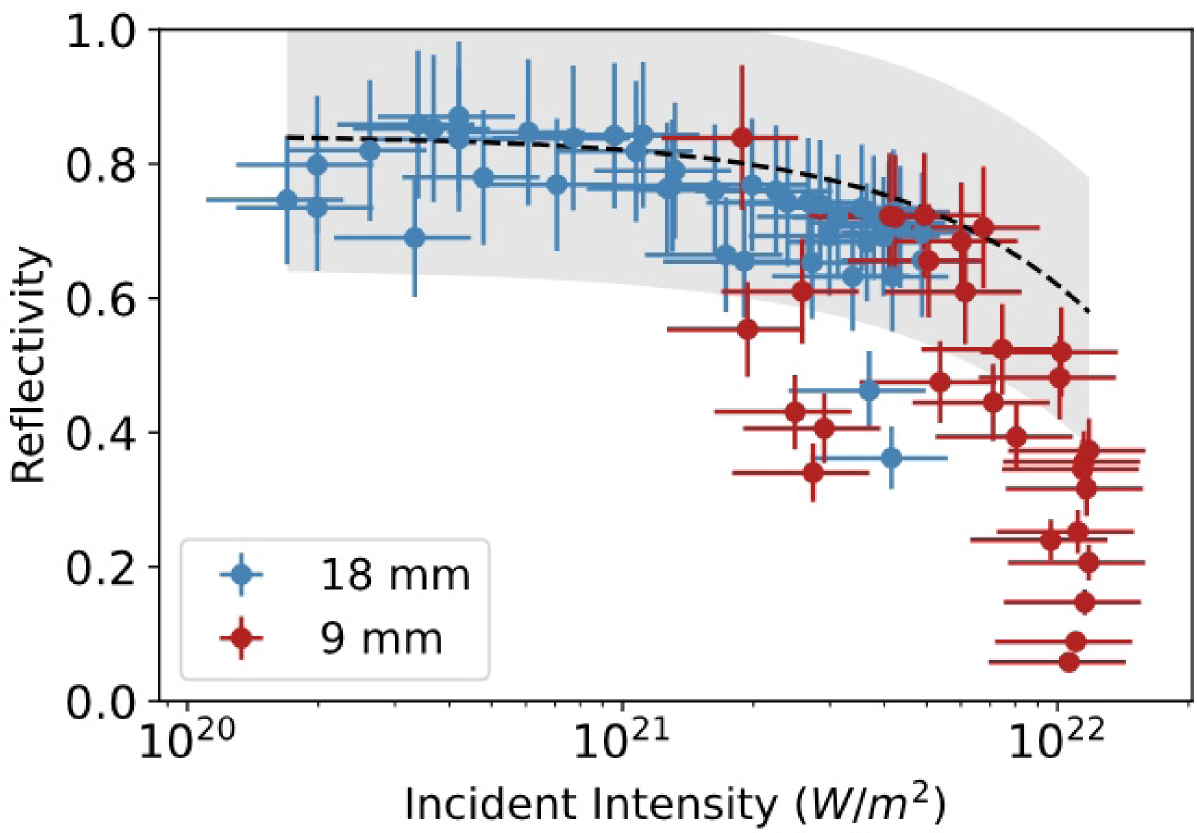

Decreasing reflectivity across incident intensities with a sharp reduction towards 10^{22} Wm^{-2}. The distances of 9 mm and 18 mm refer to the position of the tape relative to the laser focus.

Authors: J. Hills ✉, M.P. Backhouse, R. Luo, L. Kennedy, C. Cobo, E. Los, Z. Najmudin, E. Gerstmayr, J. Sarma, P. Blum, N. Lopes, N. Bourgeois, D. Bloemers, A. Thomas, S. Hawkes, S. Dann

Wakefield accelerator driven to ionisation injection using a laser reflected off a plasma mirror at high intensities

We report on a laser wakefield accelerator driven to ionisation injection using a laser pulse reflected from a thin-film plasma mirror operating at high intensities. Reflected pulses containing a maximum total energy of 3.2 ± 0.9 J were used to demonstrate a guided central spot at densities exceeding 0.5 x 10^{24} m^{-3}. Entire blue shifting of the transmitted pulse was observed between 0.5 x 10^{24} m^{-3} and 2 x 10^{24} m^{-3}. Ionisation injection was demonstrated with spots containing up to 0.4 ± 0.1 J in their FWHM at densities exceeding 2.7 ± 0.4 x 10^{24} m^{-3}.Electrons were accelerated in a cell of 6.7 ± 0.8 x 10^{24} m^{-3} to energies up to 455 ± 28 MeV using the reflected pulse. The results presented here support the utility of a tape-based plasma mirror for driving the accelerating stage of a wakefield accelerator.

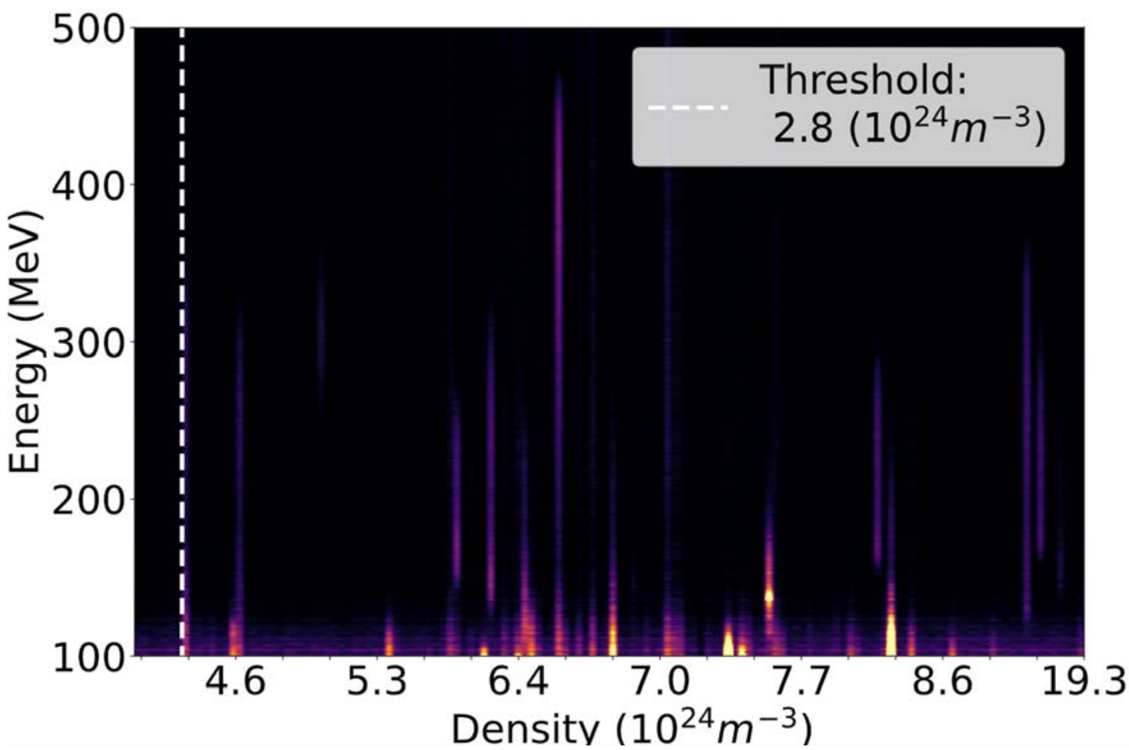

Density scan of electron spectra at different cell densities with a 10 mm long cell. Densities here are arranged in ascending order but have large uncertainties.

Authors: **J. Hills**, M.P. Backhouse, R. Luo, L. Kennedy, C. Cobo, E. Los, Z. Najmudin, E. Gerstmayr, J. Sarma, P. Blum, N. Lopes, N. Bourgeois

All-optical GeV electron bunch generation in a laser-plasma accelerator via truncated-channel injection

We describe a simple scheme, truncated-channel injection, to inject electrons directly into the wakefield driven by a high-intensity laser pulse guided in an all-optical plasma channel. We use this approach to generate dark-current-free 1.2 GeV, 4.5% relative energy spread electron bunches with 120 TW laser pulses guided in a 110 mm-long hydrodynamic optical-field-ionized plasma channel. Our experiments and particle-in-cell simulations show that high-quality electron bunches were only obtained when the drive pulse was closely aligned with the channel axis, and was focused close to the density down ramp formed at the channel entrance. Start-to-end simulations of the channel formation, and electron injection and acceleration show that increasing the channel length to 410 mm would yield 3.65 GeV bunches, with a slice energy spread ~5 x 10^{-4}.

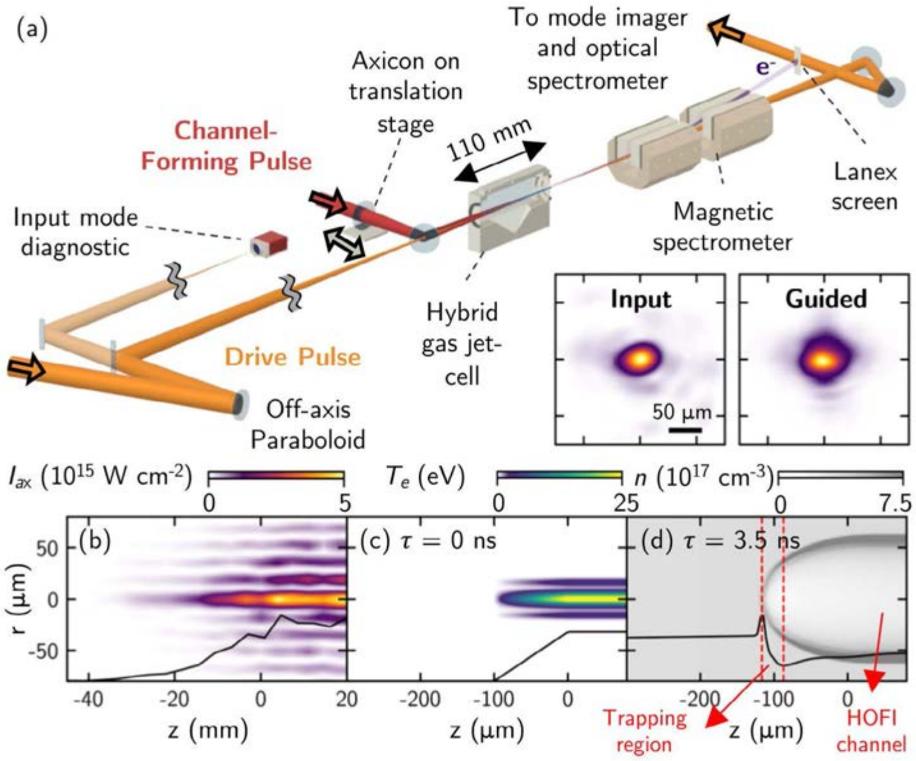

Schematic of truncated-channel injection scheme. (a) Setup: channel-forming (red) and drive (orange) beams were coupled into the gas target. The input mode, output mode, optical, and electron spectra were measured on every shot. Inset: measured transverse fluence profiles of the drive laser at focus and at the exit of the HOFI channel. (b) Measured axicon longitudinal intensity profile, (c) calculated initial electron temperature profile, and (d) calculated density profile of the truncated HOFI plasma channel 3.5 ns after arrival of the channel-forming pulse. In each panel, the black curve shows the relative magnitude of each variable along the optical axis.

Reproduced from A. Picksley et al. Phys. Rev. Lett. 131, 245001 (2023), under the terms of the **CC-BY-4.0 license**. doi: 10.1103/PhysRevLett.131.245001

Authors: A. Picksley, J. Chappell, E. Archer, N. Bourgeois, J. Cowley, D.R. Emerson, L. Feder, X.J. Gu, O. Jakobsson, A.J. Ross, W. Wang, R. Walczak, **S.M. Hooker**

Measurement of the decay of laser-driven linear plasma wakefields

We present measurements of the temporal decay rate of one-dimensional (1D), linear Langmuir waves excited by an ultrashort laser pulse. Langmuir waves with relative amplitudes of approximately 6% were driven by 1.7 J, 50 fs laser pulses in hydrogen and deuterium plasmas of density n_{e0} = 8.4 x 10^{17} cm^{-3}. The wakefield lifetimes were measured to be $\tau_{wf}^{H_2}$ = (9 ± 2) ps and $\tau_{wf}^{D_2}$ = (16 ± 8) ps, respectively, for hydrogen and deuterium. The experimental results were found to be in good agreement with 2D particle-in-cell simulations. In addition to being of fundamental interest, these results are particularly relevant to the development of laser wakefield accelerators and wakefield acceleration schemes using multiple pulses, such as multipulse laser wakefield accelerators.

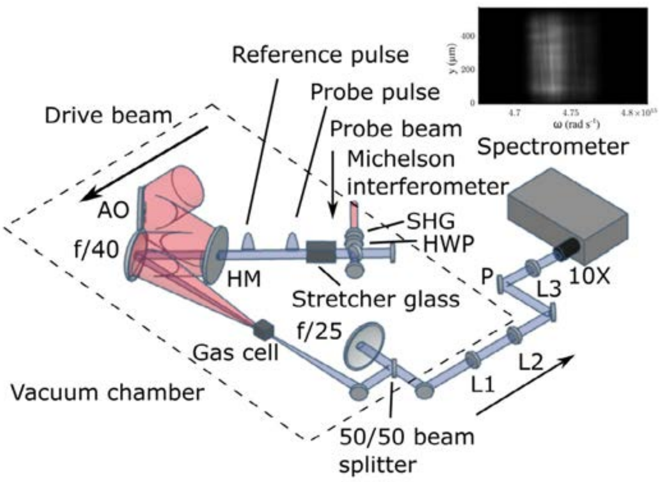

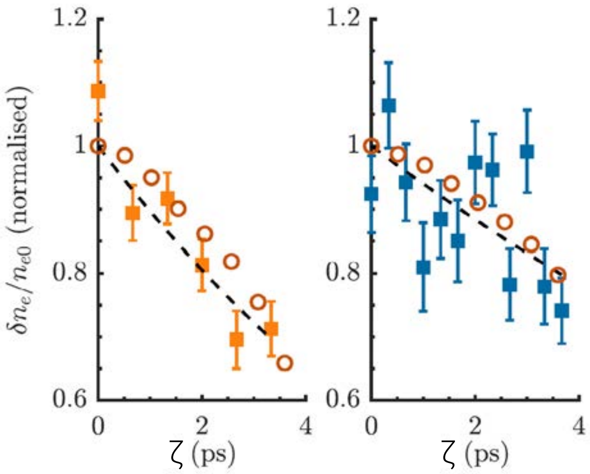

Figure 1: Schematic of the experimental layout inside the target vacuum chamber. Both beams of the Gemini TA3 laser were used: one as the drive beam, one as the diagnostic probe beam. The 800 nm beams are shown in red, and the 400 nm diagnostic beam in blue. After leaving the gas cell, the diagnostic beam was transported to a 400 nm spectrometer located outside the vacuum chamber.
Inset: example recording of a wakefield in a spectral interferogram, as captured by the spectrometer camera.
AO: Adaptive optic; HM: Holed mirror; HWP: Half-wave plate; L1: f=500 mm lens; L2: f=−100 mm lens; L3: f=300 mm lens; P: polariser; 10X: microscope objective; SHG: second harmonic generating crystal.

Figure 2: Measured normalized relative wakefield amplitude calculated using the TESS technique (see referenced paper) as a function of delay for: (a) hydrogen; (b) deuterium, recorded with a backing pressure P_{cell}=(17.0 ± 1.2) mbar. For each delay are shown the uncertainty-weighted average wakefield amplitude ($\delta n_e(\zeta)/n_{e0}$) and the standard error. The uncertainty was calculated using the background noise in the Fourier-transformed interferograms. The wakefield amplitude calculated from the PIC simulations are shown as open circles. Also shown are fits of the exponential function to the data as black lines.

Authors: J. Jonnerby, A. von Boetticher, J. Holloway, L. Corner, A. Picksley, A.J. Ross, R.J. Shalloo, C. Thornton, N. Bourgeois, R. Walczak, **S.M. Hooker** ✉

CFD modelling of gas cell target for laser wakefield accelerators

We performed 2D and 3D simulations of a gas cell target designed for laser wakefield acceleration. These are among the first full 3D simulations conducted for such a target. The simulations show that it takes a few hundred milliseconds for the density inside the cell to plateau. The cell is capable of providing density uniformity below 1%, which is a crucial factor in reducing shot-to-shot instability and improving beam quality.

The equilibrium time, based on the 3D fluid simulations, can be used to estimate the minimal delay required for the initiation of gas flow to achieve a uniform target density. The results also suggest that, for a 10 Hz LWFA, a gas cell operating in continuous mode might provide a more uniform density profile.

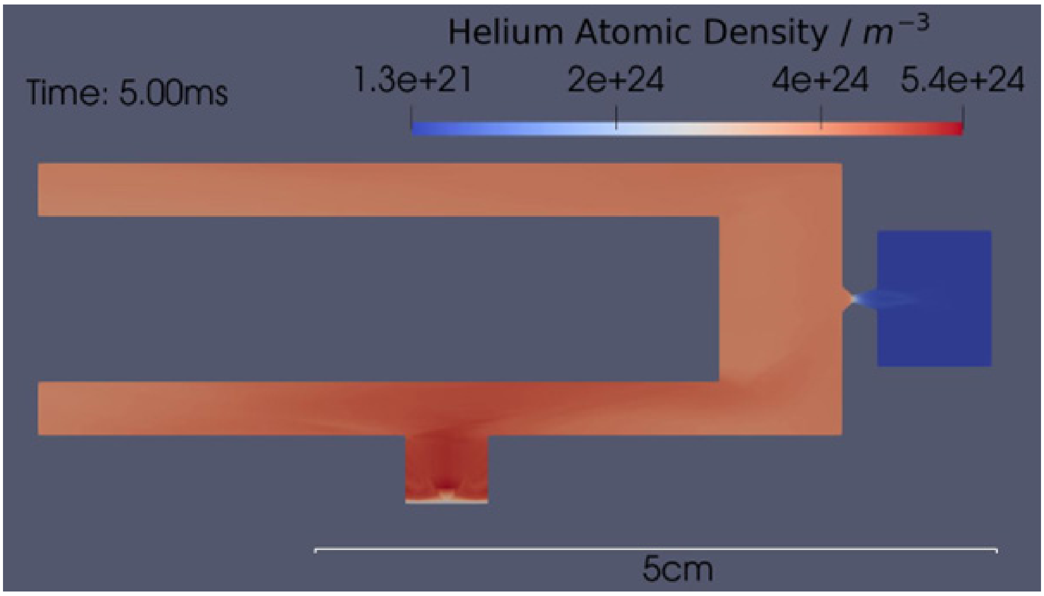

Figure 1: A transverse slice of the density distribution at 5 ms for the 3D simulation.

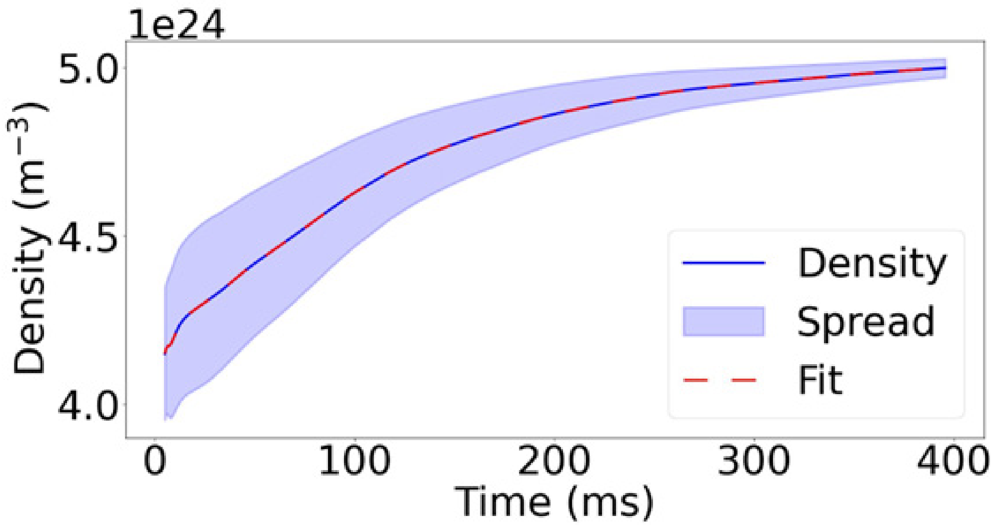

Figure 2: Mean helium atomic density evolution for in the cell for the 3D simulation.

Authors: **R. Luo**, G. Christian, J. Hills, C. Cobo, E. Los, L. Kennedy, M.P. Backhouse, Z. Najmudin, N. Lopes. P. Blum, R.J. Shalloo, E. Gerstmayr, J. Sarma, G. Sarri, N. Bourgeois

Cellular response to femtosecond-scale radiation at dose-rates exceeding 10^{13} Gy/s

We report on the characterisation of a laser driven, very high energy electron source for radiobiological applications. Here, nanocoulomb scale electron beams were generated by a laser wakefield accelerator, allowing for dose deposition up to 3 Gy per pulse. The electron beam duration is approximated to be 25 femtoseconds, equating to unprecedented single shot dose-rates in excess of 10^{13} Gy/s. The source is characterised and compared to Monte Carlo simulations, with the applications to biological research discussed.

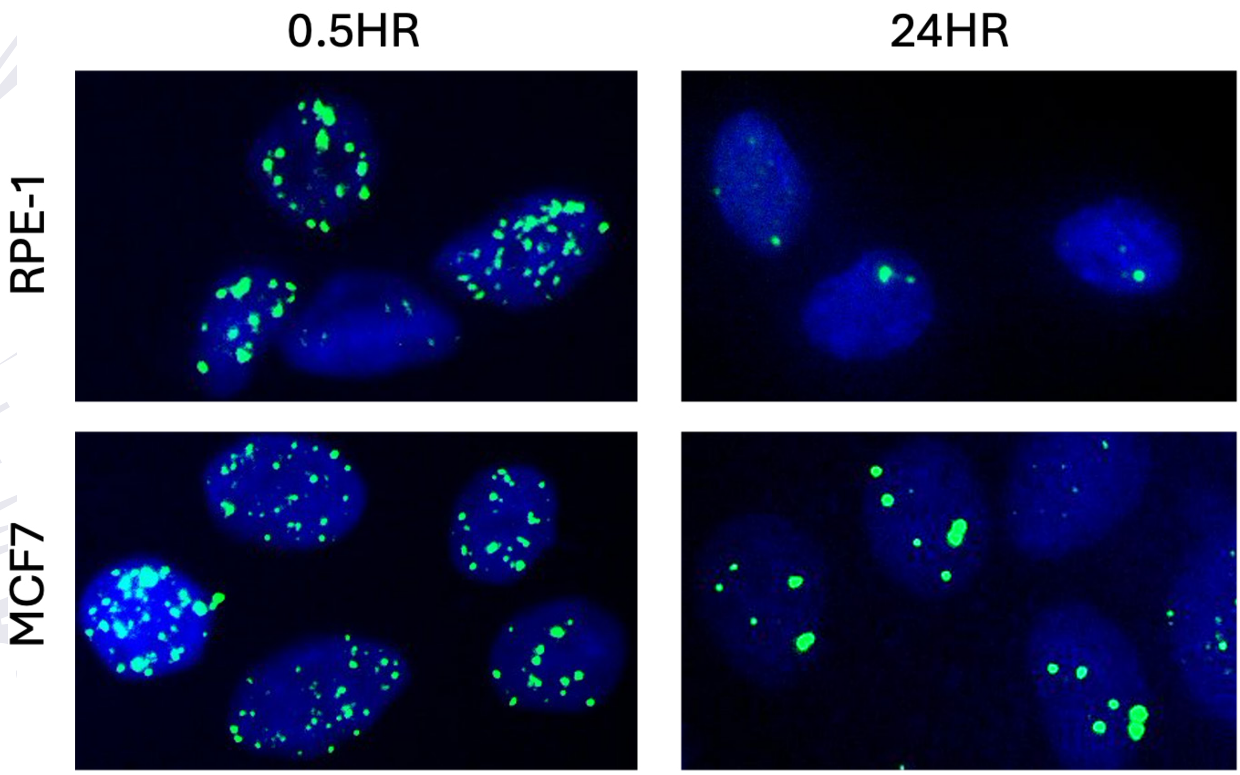

53BP1 foci formation, a DNA double strand break marker, as a function of time (0.5hr and 24hr after irradiation) for RPE-1, a healthy cell line, and MCF7, a cancerous cell line. Shown are merged channel images of 53BP1 DNA DSB marker (green) and DAPI nuclear stain (blue).

Authors: **H. Maguire** ✉, C.A. McAnespie, E. Gerstmayr, L. Calvin, J. Sarma, G. Sarri, C. McDonnell, S.J. McMahon, K.M. Prise, P. Chaudhary, G. Schettino, S.W. Botchway, S. Needham, O.J. Finlay

Monte Carlo modeling of the linear Breit-Wheeler process within the GEANT4 framework

A linear Breit-Wheeler module for the code GEANT4 has been developed. This allows signal-to-noise ratio calculations of linear Breit-Wheeler detection experiments to be performed within a single framework. The interaction between two photon sources is modelled by treating one as a static field, then photons from the second source are sampled and tracked through the field. To increase the efficiency of the module, we have used a Gaussian process regression, which can lead to an increase in the calculation rate by a factor of up to 1000. To demonstrate the capabilities of this module, we use it to perform a parameter scan, modelling an experiment based on that recently reported by Kettle et al. [New J. Phys. 23, 115006 (2021)]. We show that colliding 50-fs duration γ rays, produced through bremsstrahlung emission of a 100 pC, 2-GeV laser wakefield accelerator beam, with a 50-ps x-ray field, generated by a germanium burn-through foil heated to temperatures >150 eV, this experiment is capable of producing > 1 Breit-Wheeler pair per shot.

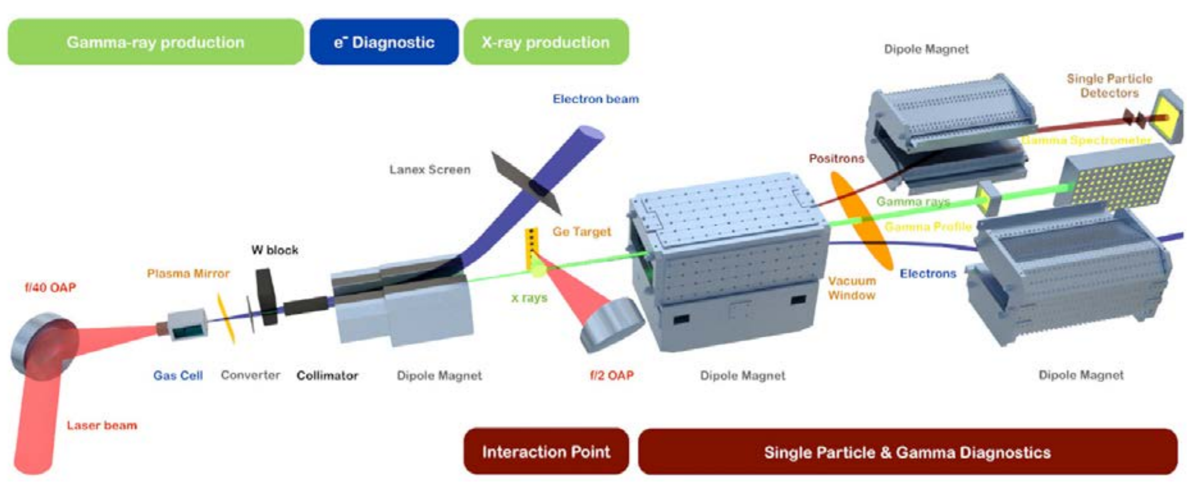

Schematic of Gemini linear Breit-Wheeler (BW) detection experiment. Starting from the left: a LWFA generates an electron beam which is converted into a gamma ray beam through bremsstrahlung emission in a thin bismuth converter foil. A tungsten collimator and block are placed in the beam path to remove highly divergent gamma rays and those directed toward the x-ray foil, respectively. A large number of Bethe-Heitler (BH) pairs are produced in the converter foil, collimator, and block. These are removed with an on-axis magnet before the interaction zone. The gamma rays interact with an x-ray field, generated by a laser heated germanium foil, producing BW pairs. The residual gamma rays continue on axis to a spectrometer. The BW pairs pass through a magnetic chicane to single particle detectors, situated behind lead shielding (not shown). Diagram provided by Gerstmayr.

Reproduced from S.P.D. Mangles et al. Phys. Rev. Accel. Beams 26, 054601 (2023), under the terms of the **CC-BY-4.0 license**. doi: 10.1103/PhysRevAccelBeams.26.054601

Authors: R.A. Watt, S.J. Rose, B. Kettle, **S.P.D. Mangles**

Narrow bandwidth, low-emittance positron beams from a laser-wakefield accelerator

The rapid progress that plasma wakefield accelerators are experiencing is now posing the question as to whether they could be included in the design of the next generation of high-energy electron positron colliders. However, the typical structure of the accelerating wakefields presents challenging complications for positron acceleration. Despite seminal proof-of-principle experiments and theoretical proposals, experimental research in plasma-based acceleration of positrons is currently limited by the scarcity of positron beams suitable to seed a plasma accelerator. Here, we report on the first experimental demonstration of a laser-driven source of ultra-relativistic positrons with sufficient spectral and spatial quality to be injected in a plasma accelerator. Our results indicate, in agreement with numerical simulations, selection and transport of positron beamlets containing $N_{e+} \geq 10^5$ positrons in a 5% bandwidth around 600 MeV, with femtosecond-scale duration and micron-scale normalised emittance. Particle-in-cell simulations show that positron beams of this kind can be guided and accelerated in a laser-driven plasma accelerator, with favourable scalings to further increase overall charge and energy using PW-scale lasers. The results presented here demonstrate the possibility of performing experimental studies of positron acceleration in a laser-driven wakefeld accelerator.

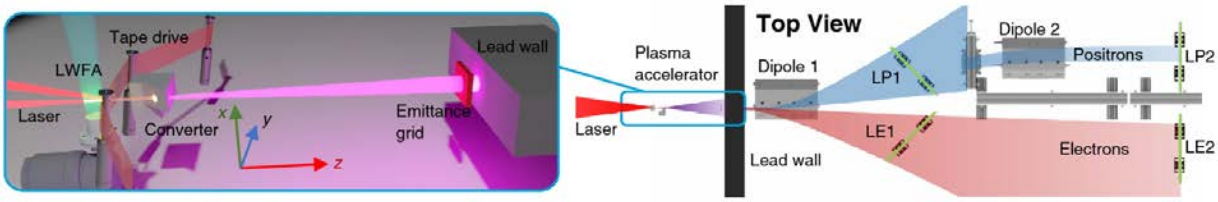

Figure 1: Illustration of the experimental setup, showing the electron plasma accelerator, the converter, the emittance mask, scintillators for electrons (LE1 and LE2) and positrons (LP1 and LP2). Electron (red) and positron (blue) trajectories are also shown to guide the eye.

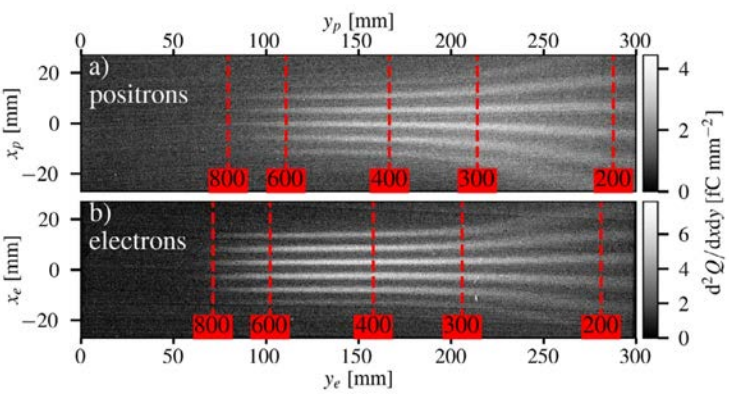

Figure 2: Raw images of energy-resolved beam profiles with the emittance mask. Example modulated (a) positron and (b) electron spatial charge density as a function of position on the screens (xp, yp, xe, ye) for a single shot with a converter thickness of 8.0 mm and the emittance mask in the beam-line. Vertical red dashed lines indicate positions corresponding to the given particle energies in MeV. The difference between electron and positron raw data is due to the slightly different position of the scintillator screens (see published paper).

Reproduced from M.J.V. Streeter, C. Colgan, J. Carderelli et al. Narrow bandwidth, low-emittance positron beams from a laser-wakefield accelerator. Sci Rep 14, 6001 (2024),
 doi: 10.1038/s41598-024-56281-1

Authors: M.J.V. Streeter, C. Colgan, J. Carderelli, Y. Ma, N. Cavanagh, E.E. Los, H. Ahmed, A.F.Antoine, T. Audet, M.D. Balcazar, L. Calvin, B. Kettle, S.P.D. Mangles, Z. Najmudin, P.P. Rajeev, D.R. Symes, A.G.R. Thomas, **G. Sarri** ✉

Measurement of magnetic cavitation driven by heat flow in a plasma

Experiments at Vulcan TAW led to direct measurements of the dynamics of magnetic fields driven by heat flow in a plasma. In ideal plasma, field lines are considered to be locked to the bulk motion ('frozen in flow'), but we measured that the magnetic field was instead expelled from a hot plasma much faster than the plasma could move. This Nernst advection is driven by electron heat conduction occurring on the timescale of a few 100s ps, whereas bulk plasma motion is limited by heavier ions, which take longer to respond.

By making these measurements of magnetic field advection we demonstrated a new way of studying heat flow in hot magnetised plasmas. We showed that while the hydrodynamic motion is insufficient to explain the magnetic field dynamics, extended MHD simulations do a surprisingly good job of modelling the advection process because the magnetic field effectively localises the heat flow.

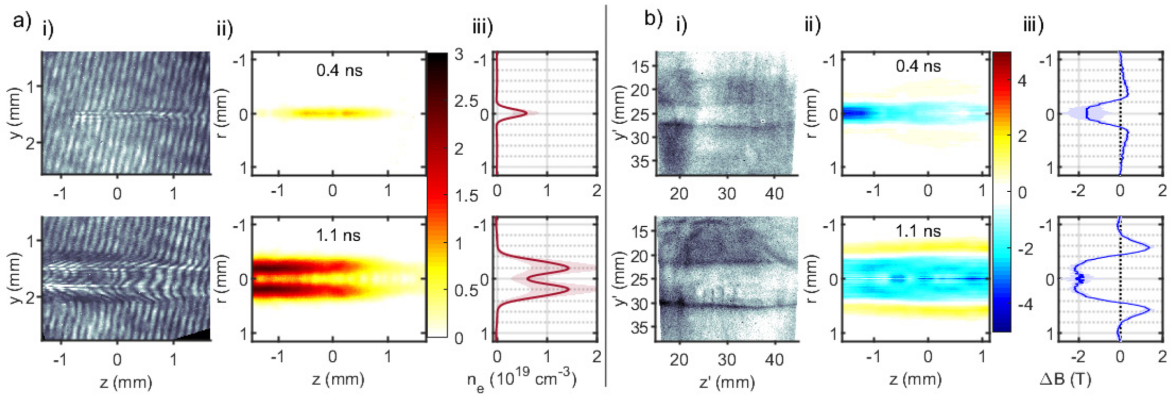

Figure 1 (from doi: 10.1103/PhysRevLett.131.015101): Results from a) optical interferometry, measuring electron density and b) proton radiography, measuring change in the magnetic field. (i) Raw data for two different shots taken under the same conditions, one 0.4 ns after the start of the heater beam and one 1.1 ns after the start. (ii) The plasma column and cavity in the magnetic field both expand over time, with the longitudinally averaged profiles (iii) showing how the cavity remains larger than the plasma column throughout.

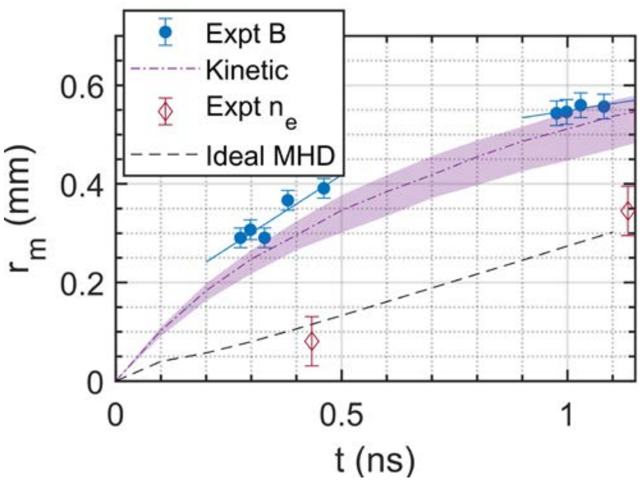

Figure 2: The position of the peak in the magnetic field over time (blue circles), compared with the position of the HWHM of the plasma density (red open diamonds). Overlaid are the positions predicted from simulations, showing how kinetic simulations (dash-dotted) do a good job of predicting the magnetic field dynamics, whereas ideal MHD predicts much slower advection tied to the motion of the plasma (frozen-in-flow).

Authors: **C. Arran** ✉, P. Bradford. A. Dearling, G.S. Hicks, S. Al-Atabi, L. Antonelli, O.C. Ettlinger, M. Khan, M.P. Read, K. Glize, M. Notley, C.A. Walsh, R.J. Kingham, Z. Najmudin, C.P. Ridgers, N.C. Woolsey

Proton beam divergence measurements from radiation pressure driven shock acceleration

Laser-plasma ion acceleration is a fast-developing field of research, yielding ion sources capable of generating high energy, high current, short ion beams. These characteristics make them ideally suited to many applications, including hadron radiation therapy and nuclear physics. We performed a radiation driven, front surface ion acceleration experiment using a long wavelength CO_2 laser to irradiate gas targets. We devised and fielded a proton spatial diagnostic which enabled us to make novel measurements of ion beam divergence. By comparison with shadowgraphy, we observed a relationship between the emission angle of the energetic ions and the electrons generated in the laser plasma interaction. We also observed spatial and spectral modulations of the proton beam on our ion diagnostics.

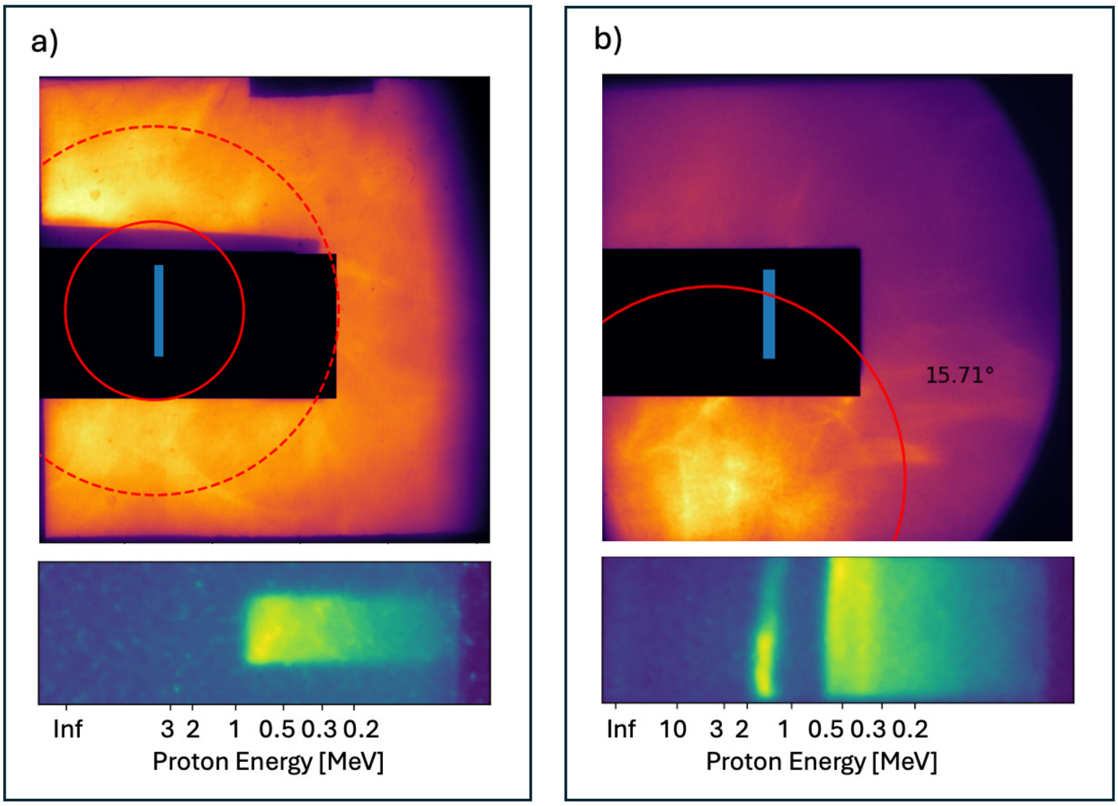

Representative proton spatial (top) and Thompson spectrometer data (bottom) for two different acceleration modes. The blue region on both scintillator images shows where the Thompson parabola's slit is located spatially. The red circles in a) show the 10° and 20° beam divergence boundaries, in b) the red circle shows the FWHM of the ion beam obtained by fitting Gaussians. Laser energies were 5 J for both shots, the pre-pulse was 5 mJ in a) and 40 mJ in b).

Authors: G. Casati ✉, N.P. Dover, O.C. Ettlinger, C.A.J. Palmer, I. Pogorelsky, M. Polyanskiy, N. Xu, W, Li, M. Babzien, Z. Najmudin

Optimizing laser coupling, matter heating, and particle acceleration from solids using multiplexed ultra-intense lasers

This paper uses laboratory experiments and detailed numerical simulations to investigate how to optimise the coupling of multi-petawatt (PW) class lasers onto solid targets. We show, in brief, that stacking beams side-by-side to irradiate a target in a mirror-like configuration gives rise to an enhanced absorption and injection of fast electrons in the target. This is due to magnetic reconnection taking place between the magnetic fields induced by each laser, which thus generates an electric field that boosts the generation of electrons. Further, we show that this induces a virtuous cascade, because the enhanced electron injection can benefit from self-induced enhanced transport through the target. Thus, we show that physics can be advantageously exploited to improve particle acceleration compared to the mere addition of several lasers onto a target.

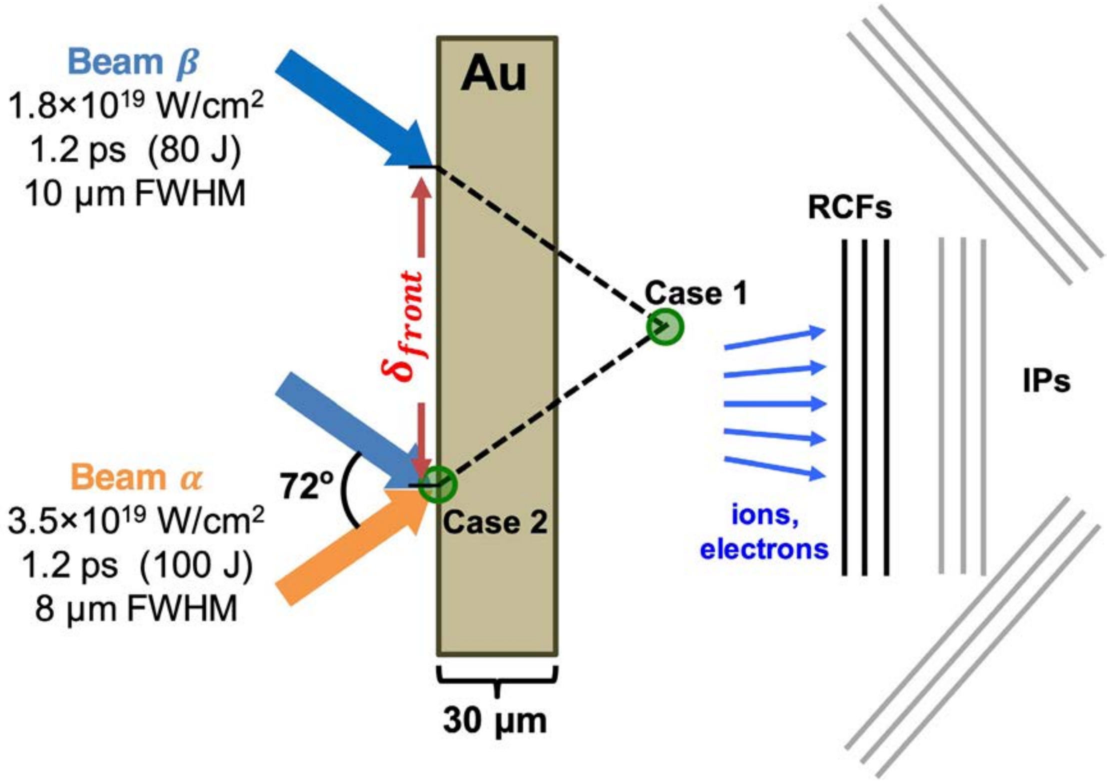

Schematic of the experiment, using two intense laser beams irradiating a solid gold target with opposite incidence angles and a variable separation distance between the laser spots on the target front surface. In all cases, the focus of the laser beams coincides with the target surface. The outgoing hot electrons are diagnosed by image plate (IP) stacks, located along each laser beam axis, as well as in the target normal direction. The accelerated ions are characterized by a radiochromic film (RCF) stack located in the target normal direction.

Further details can be found in W. Yao et al., Matter Radiat. Extremes 9, 047202 (2024). doi: 10.1063/5.0184919

Authors: **W. Yao** ✉, M. Nakatsutsumi, S. Buffechoux, P. Antici, M. Borghesi, A. Ciardi, S. Chen, E. d'Humières, L. Gremillet, R. Heathcote, V. Horný, P. McKenna, M. Quinn, L. Romagnani, R. Royle, G. Sarri, Y. Sentoku, H.-P. Schlenvoigt, T. Toncian, O. Tresca, L. Vassura, O. Willi, J. Fuchs